

- ⁴A. Ascoli, *J. Inst. Metals* **89**, 218 (1961).
⁵G. V. Kidson, *Phil. Mag.* **13**, 247 (1966).
⁶C. Wagner, *Z. Physik Chem. (Frankfurt)* **38**, 325 (1957).
⁷A. Ascoli and A. C. Damask, *Bull. Am. Phys. Soc.* **5**, 182 (1960).
⁸F. C. Frank and D. Turnbull, *Phys. Rev.* **104**, 617 (1956).
⁹H. R. Curtin, D. L. Decker, and H. B. Vanfleet, *Phys. Rev.* **139**, A1552 (1965).
¹⁰B. F. Dyson, T. Anthony, and D. Turnbull, *J. Appl. Phys.* **37**, 2370 (1966).
¹¹N. H. Nachtrieb, H. A. Resing, and S. A. Rice, *J. Chem. Phys.* **31**, 135 (1959).
¹²J. B. Hudson and R. E. Hoffman, *Trans. Met. Soc. AIME* **221**, 761 (1961).
¹³A. Ascoli, B. Bollani, G. Guarini, and D. Kustudic, *Phys. Rev.* **141**, 732 (1966).
¹⁴S. A. Rice and N. H. Nachtrieb, *J. Chem. Phys.* **31**, 139 (1959).
¹⁵E. Rapoport, *J. Chem. Phys.* **44**, 3581 (1966).
¹⁶D. L. Decker, *Rev. Sci. Instr.* **39**, 603 (1968).
¹⁷These values are typical up-cycle transition pressures for the Bi I-II and Tl II-III as measured by H. B. Vanfleet and R. J. Zeto (unpublished) using a manganin gauge in a hydrostatic-pressure cell.
¹⁸R. E. Hannenan, H. M. Strong, and F. P. Bundy, in *Accurate Characterization of the High Pressure Environment*, edited by E. C. Lloyd (U.S. GPO, Washington, D. C., 1971).
¹⁹I. C. Getting and G. C. Kennedy, *J. Appl. Phys.* **41**, 4552 (1970).
²⁰C. Y. Wang, *Rev. Sci. Instr.* **38**, 24 (1967).
²¹R. K. Young, Ph.D. dissertation (Brigham Young University, 1969) (unpublished).
²²J. A. Weyland, Ph.D. dissertation (Brigham Young University, 1969) (unpublished).
²³R. N. Jeffery and D. Lazarus, *J. Appl. Phys.* **41**, 3186 (1970).
²⁴L. W. Barr, J. N. Mundy, and F. A. Smith, *Phil. Mag.* **20**, 389 (1969).
²⁵R. A. Miller and D. E. Schuele, *J. Phys. Chem. Solids* **30**, 589 (1969).
²⁶F. C. Nix and D. MacNair, *Phys. Rev.* **61**, 74 (1941).
²⁷L. E. Millet, Ph.D. dissertation (Brigham Young University, 1968) (unpublished).
²⁸R. E. Hanneman and H. M. Strong, *J. Appl. Phys.* **36**, 523 (1965).
²⁹H. M. Gilder (private communication).
³⁰T. R. Anthony, B. F. Dyson, and D. Turnbull, *J. Appl. Phys.* **37**, 2925 (1966).
³¹C. Zener, *J. Appl. Phys.* **22**, 372 (1951).

Theory of Work-Function Changes Induced by Alkali Adsorption

N. D. Lang

IBM Thomas J. Watson Research Center, Yorktown Heights, New York 10598

(Received 28 December 1970; revised manuscript received 19 August 1971)

Changes of the work function due to adsorption of alkali atoms by a high-work-function substrate are studied using a very simple ("jellium") model of the metallic substrate-adsorbate system. A self-consistent quantum-mechanical analysis of the model leads to a work-function-vs-coverage curve with a minimum at a coverage below that of a single full adsorbed layer, and a maximum at completion of the layer. Good agreement with the results of recent measurements is obtained for these extremal values; and, though not designed to treat very low coverages, the model yields an initial dipole moment in satisfactory agreement with experiment. The computed full-layer work function is very nearly equal to that obtained theoretically for the corresponding bulk sample. A study of limiting cases provides a framework for viewing the results of the calculation in a coherent way.

I. INTRODUCTION

As alkali metal atoms are adsorbed onto the surface of a metal such as W or Ni, the measured work function decreases rapidly from its initially high value. With continued adsorption, the work function reaches a minimum, and then rises to approximately the bulk alkali value with completion of the first full layer of adsorbate atoms.

Some of the earliest observations of this behavior were reported by Ives,¹ Langmuir and Kingdon,² and Becker.³ Since the time of this early work, there have been many such experimental studies. One of the chief reasons for this effort stems from

interest in alkali adsorption as a way of enhancing the electron-emission properties of a surface. Another is the strong theoretical interest in this process as one of the simplest examples of chemisorption.

The first explanation for these observed changes of work function appears to be due to Langmuir.⁴ His picture is as follows: When the alkali atoms are adsorbed, they lose their valence electrons to the substrate. (This loss was ascribed to the fact that the adatom ionization potential is less than the substrate work function.) The resulting positive ions induce images in the substrate, producing dipoles which lower the work function by an amount

proportional to pN , with p the magnitude of the dipole moment per adatom, and N the number of adatoms per unit area. Each dipole, however, is depolarized by the electric field due to all the others: The greater the coverage (N), the greater the depolarization. The minimum in the work-function-vs-coverage curve occurs when the relative decrease in dipole moment per adatom (dp/p) balances the relative increase in the number of dipoles (dN/N). This picture, while conceptually useful, is not satisfactory in a detailed way. The alkali atoms are not completely ionized, the image approximation breaks down at very short distances, and it is difficult to assign a polarizability to the dipoles.

A more quantum-mechanically oriented model was proposed by Gurney.⁵ The adsorbed atom is viewed as having a valence-electron energy level which lies in the vicinity of the substrate Fermi energy and which is broadened because of the presence of the substrate. The degree of ionization, and hence (for some particular distance of charge separation) the strength of the dipole moment per adatom, is determined by the fractional occupation of this broadened level, which in turn depends upon the position of the level relative to the Fermi energy. Increases in coverage cause "depolarization" by lowering the surface potential, and hence the level position. As before, changes in p and N lead to changes in the work function. This model, though theoretically more satisfying than that introduced by Langmuir, involves a good deal of complexity in actual application. It is most useful at very low coverages, for which adatom-adatom interactions are small. Even in this regime, however, determination of the parameters of the adatom-substrate interaction can be quite difficult.

This picture has been employed by several writers⁶⁻¹² in recent studies of the chemisorption of a single alkali atom on a metal surface. Some work has been done in extending these treatments away from the single-adatom case,¹³ but there appear to be no first-principles analyses for other than very low coverages.¹⁴

The present treatment is based on the theory of the inhomogeneous electron gas,¹⁵ and uses techniques employed earlier for the study of bare metal surfaces.¹⁶⁻¹⁹ The substrate ionic lattice is replaced by a semiinfinite uniform positive background, and the array of adsorbate ions by an adjoining uniform positive slab. The electron density associated with this positive charge configuration is obtained through a self-consistent wave-mechanical calculation, and from this density the work function for the model follows immediately. Changes in coverage are treated as changes in the density of the adsorbate background slab.²⁰

This study represents an approach very different

from that of the quantum-mechanical analyses cited above, in that it attempts to treat a considerably simpler model much more exactly. The calculations give a good quantitative account of recent experimental data, and the model is seen to provide a simple framework for understanding, in terms of limiting cases, the general features of the results.

II. UNIFORM-BACKGROUND MODELS

A. Bare Surface

Since the model proposed for alkali adsorption is a simple extension of one employed earlier for the bare surface, it is most useful to begin our discussion with a summary of the relevant aspects of this earlier work.

References 16 and 17 considered the problem of determining the electronic charge distribution in the surface region of a model of a metal in which the ionic lattice is replaced by a uniform positive charge background of density:

$$n_+(\vec{r}) = \begin{cases} \bar{n}_{\text{sub}}, & x \leq 0 \\ 0, & x > 0 \end{cases} \quad (2.1)$$

(The reason for the "sub" will become evident below.) The electron density $n(x)$ was found by solving self-consistently a set of one-particle equations introduced by Kohn and Sham.¹⁵ The potential appearing in these equations is a sum of the electrostatic potential $\phi(x)$ due to the positive background and to the electrons, and what may be called an effective exchange-correlation potential. Just as in Refs. 16 and 17, all terms in the exchange-correlation potential involving gradients of the density were omitted.

In Ref. 18, the work function Φ was shown, in general, to be given by

$$\Phi = \Delta\phi - \bar{\mu}, \quad (2.2)$$

where $\bar{\mu}$ is the bulk chemical potential of the electrons relative to the mean electrostatic potential in the metal interior, and $\Delta\phi$ is the rise in mean electrostatic potential across the metal surface. For the simple model introduced above, $\bar{\mu}$ is a function only of \bar{n}_{sub} , and $\Delta\phi$ is, from Poisson's equation,²¹

$$\Delta\phi = \phi(\infty) - \phi(-\infty) = 4\pi \int_{-\infty}^{\infty} dx x [n(x) - n_+(x)]. \quad (2.3)$$

Over roughly the metallic range of densities, i. e., the range $r_s^{(\text{sub})} = 2-6$ a. u. [with $\frac{4}{3}\pi(r_s^{(\text{sub})})^3 \equiv (\bar{n}_{\text{sub}})^{-1}$], the Φ computed for this model changes in a way approximately linear in $r_s^{(\text{sub})}$, from 3.9 eV at $r_s^{(\text{sub})} = 2$ to 2.4 eV at $r_s^{(\text{sub})} = 6$.^{16, 18} Good agreement is obtained with experimental data on the work functions of polycrystalline simple metals: the alkalis and polyvalent metals such as Al and Mg.^{16, 18} The model in the form described here does not yield the generally higher work functions found for the noble and transition metals.²²

References 17 and 18 go on to consider a more realistic model of the metal, in which the effect of each metal ion on the conduction electrons is represented by an appropriate pseudopotential. This reintroduction of the ionic lattice into the model may be viewed as the addition to the Hamiltonian of a perturbing potential $\delta v(\vec{r})$, equal to the difference between the total pseudopotential (of all the ions) and the potential due to the uniform positive background. Since δv is small (for the simple metals), first-order perturbation theory can be used to determine the influence of the lattice on the work function. This permits, in particular, a study of work-function anisotropy.¹⁸

In order that $\delta v(\vec{r})$ have no mean slope at $\pm\infty$, the lattice planes are taken to be at $x = -\frac{1}{2}d_{\text{sub}}, -\frac{3}{2}d_{\text{sub}}, \dots$, where d_{sub} is the interplanar spacing²³ (recall that the positive background fills the region $x \leq 0$). Accordingly, we may view the uniform-background model as a smearing out of the ionic charge in each lattice plane into a uniform slab of thickness d_{sub} centered about the plane. This plane-by-plane replacement of the ions by slabs of positive charge is extended below to obtain a simple model for alkali chemisorption.

B. Surface with Adsorbed Layer

In our study of alkali adsorption on metals, we represent the substrate by using the semiinfinite uniform-background model described above. To provide a rough simulation of the fact that most of the experiments are done on substrates of high work function (usually transition metals), \bar{n}_{sub} will be taken at the $r_s^{(\text{sub})} = 2$ end of the metallic range (where $\Phi \approx 4$ eV). The exact value of the substrate work function is found to have relatively little influence on the quantities we wish to consider (see below), and so the fact that transition-metal work functions are frequently of the order of 5 rather than 4 eV is disregarded in our analysis.

In just the same way that we replaced the planes of ions in the bare-surface model by charge slabs, we here replace the ionic charge of the adsorbate layer by a homogeneous positive slab²⁴ of thickness d and density \bar{n} , immediately adjoining the substrate background (we consider for now single- rather than multiple-layer coverage). Thus the total positive background configuration in our adsorption model is

$$n_+(x) = \begin{cases} \bar{n}_{\text{sub}} & , \quad x \leq 0 \\ \bar{n} & , \quad 0 < x \leq d \\ 0 & , \quad x > d \end{cases} \quad (2.4)$$

[This implies that, were we to reintroduce the effects of the ions (by using perturbation theory, for example), the separation between the first substrate lattice plane and the layer of adsorbate ions would be $\frac{1}{2}(d + d_{\text{sub}})$.²⁵] Since the alkalis are monovalent,

$$\bar{n}d = N, \quad (2.5)$$

with N the number of alkali atoms per unit area. Changes in coverage N can be represented by changes in either \bar{n} or d (or both). We will make the extremely simple choice of taking d to have some fixed value for each alkali (which is equivalent to neglecting variations in the substrate-adsorbate ionic separation), and will change only \bar{n} .²⁶

Experimentally, it is found that a second layer of alkali atoms begins to form when N reaches a value roughly equal to N_A , the number of atoms per unit area in the most densely packed lattice planes of a bulk sample of alkali A ($A = \text{Li}, \text{Na}, \text{etc.}$).^{27,28} This suggests that a reasonable choice for d might then be the bulk value of the spacing of these planes²⁶ (implying that \bar{n} for a full layer would be roughly the same as in the bulk²⁹). This choice will be regarded as a convenient starting point for discussion; its adequacy will be examined in Sec. III. These particular d values will be denoted d_A ³⁰; and the mean electron density (or mean ionic charge density) for the bulk alkali will be denoted \bar{n}_A .

To find the work function for our substrate-adsorbate model, we proceed in exactly the same way that we did for the bare surface. We begin with the positive charge configuration given in Eq. (2.4), add enough electrons to produce charge neutrality, and calculate self-consistently the density distribution $n(x)$ of these electrons. The only computational difference occurs in the form of the electrostatic potential $\phi(x)$ that enters the one-particle equations, since $n_+(x)$ now has a somewhat different form (this, however, is a trivial difference). Once we know $n(x)$, we find Φ by using Eq. (2.2) (μ is the same as before).

It is clear that our model is not designed to treat the case of very low coverages: The replacement of an array of adsorbate ions by a continuous positive charge distribution is a more severe approximation the sparser the ionic array. In this sense the model is complementary to that of Refs. 5-11. There are, however, reasons why we should still obtain reasonable results even at low coverages for the work-function change due to adsorption (see the Appendix).

C. Computations

For each of four choices of d ($d_{\text{Li}}, d_{\text{Na}}, d_{\text{K}}, d_{\text{Cs}}$), a range of \bar{n} values between zero and \bar{n}_A was considered. The electron density distribution $n(x)$ was computed self-consistently for each \bar{n} , and from this, the corresponding Φ was calculated as described above. In this way, curves of Φ vs \bar{n} were obtained for these several values of d . The behavior of Φ at other intermediate d values can be found by interpolation.

Figure 1 shows $n(x)$ for the case $d = d_{\text{Na}}$ and

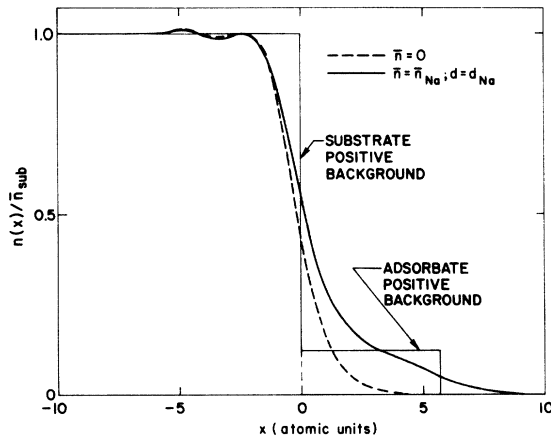


FIG. 1. Self-consistent electron density distributions $n(x)$ for bare-substrate model ($\gamma_s^{(\text{sub})} = 2$) and for model of substrate with a full layer of adsorbed Na atoms.

$\bar{n} = \bar{n}_{\text{Na}}$, as well as for the case of the bare substrate ($\gamma_s^{(\text{sub})} = 2$). Figure 2 gives Φ curves for $d = d_{\text{Na}}$ and $d = d_{\text{Cs}}$. The abscissa in this figure is not \bar{n} but the more physically meaningful quantity N .

The most important fact about the curves in Fig. 2 is that they do indeed exhibit a minimum. In addition, they illustrate the experimentally observed trend along the series Li, Na, K, Cs (no recent data were found for Rb) of a decrease in both the minimum work-function value (Φ_{min}) and coverage²⁷ at which the minimum occurs (N_{min}). Theoretical reasons for this trend and for the existence of the minimum are discussed in Sec. IV.

Before proceeding to a comparison of our results with those of experiment, it is convenient to consider what would happen if the adsorbate positive background slab in our model were to be displaced away from the substrate background, that is, if the $n_+(x)$ of Eq. (2.4) were to be replaced by

$$n_+(x) = \begin{cases} \bar{n}_{\text{sub}}, & x \leq 0 \\ 0, & 0 < x \leq \Delta \\ \bar{n}, & \Delta < x \leq d + \Delta \\ 0, & x > d + \Delta \end{cases} \quad (2.6)$$

with $\Delta > 0$. It is useful, for purposes of discussion, to focus on a specific case. If we translate an adsorbate slab of thickness d_{Na} so that its center lies at the same position as the center of an untranslated slab of thickness d_{Cs} [i. e., if we take $\Delta = \frac{1}{2}(d_{\text{Cs}} - d_{\text{Na}})$], then will the results for $\Phi(N)$ resemble most closely those of Na or those of Cs? This question can be answered simply by recalling that a slab of positive charge in our model represents a sheet of ions (with appropriate pseudopotential cancellation) at its center.²⁸ We expect therefore that the $\Phi(N)$ curve for the case posed here will be most like that for Cs, which is seen in fact to be the case (dashed curve

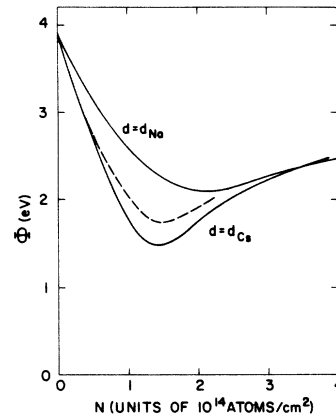


FIG. 2. Calculated $\Phi(N)$ curves for Na and Cs adsorption. Cs curve terminates at N_{Cs} (N_{Na} is off scale). Dashed curve is explained in text. Values of N_{min} indicated here are substantially smaller than those determined for adsorption on a substrate such as W(110), whose Φ_{sub} is much larger than that of the model. The values of quantities such as Φ_{min} , by contrast, are relatively independent of Φ_{sub} (see text).

in Fig. 2).

III. COMPARISON BETWEEN THEORY AND EXPERIMENT

A. General Remarks

In drawing comparisons between theory and experiment, we will use only data for adsorption on the most densely packed crystal face of the substrate, since this face presents to the adsorbate an electron density most like that of our simple model, with its absence of variation parallel to the surface.²² Since the work function of our substrate is fixed at 3.9 eV, while most experiments employ substrates with work functions close to 5 eV, we shall not compare $\Phi(N)$ curves directly. [The comparison of curves of $\Phi(N) - \Phi(0)$ is not useful either, as will be seen presently.] Instead, we shall com-

TABLE I. Experimental data for Cs adsorption illustrating the fact that Φ_{min} is not strongly dependent on Φ_{sub} (see text). Measurements on polycrystalline substrates are by Swanson and Strayer (Ref. 31); those on single-crystal faces of W are by Gavriljuk, Naumovets, and Fedorus (Ref. 32).

Substrate	Φ_{sub} (eV)	Φ_{min} (eV)
Mo (polycrystalline)	4.20	1.54 ± 0.05
W (polycrystalline)	4.52	1.52 ± 0.05
Re (polycrystalline)	4.85	1.45 ± 0.05
Ni (polycrystalline)	5.00	1.37 ± 0.05
W(111)	4.4	1.5
W(100)	4.55	1.35
W(112)	4.8	1.55
W(110)	5.4	1.5

pare only those features of the curves which are found to be relatively independent of $\Phi_{\text{sub}} \equiv \Phi(0)$: These are the values of Φ_{min} , $\Phi'(0) \equiv d\Phi/dN$ at $N=0$, and Φ for a single full layer of adsorbed atoms. Theoretical evidence suggesting this independence is given in Sec. IV. Clear experimental evidence, on the other hand, appears to be available just for Φ_{min} [the experimental study of $\Phi'(0)$ and of Φ for a full layer involves certain problems which are discussed below].

Some of the data showing that Φ_{min} is only weakly dependent on Φ_{sub} are given in Table I. The upper half of the table gives Φ_{min} as measured by Swanson and Strayer³¹ for Cs adsorption on polycrystalline Mo, W, Re, and Ni (single-crystal data for all of these substrates were not available). While the work functions of the substrates cover a range of 0.8 eV, the corresponding Φ_{min} values exhibit a spread of only 0.17 eV.

Since Cs is the largest alkali atom, it should be least sensitive to variations in the packing density among the different substrate crystal faces (particularly away from the very low coverages at which the adatoms are most strongly ionized). It is partly for this reason that our use here of polycrystalline data is justified. By the same token, we should also be able to consider data for Cs adsorption on different crystal faces of the same substrate (these faces have different work functions). The lower half of Table I gives results of Gavriljuk, Naumovets, and Fedorus³² for faces of W whose work functions are spread over a 1-eV range. The Φ_{min} values are seen to differ by at most 0.2 eV.

We observe at this point that there is no evidence for considering N_{min} to be independent of Φ_{sub} ; in fact both theory³³ and experiment³² suggest the contrary. Hence we note that only the N_{min} values obtained theoretically (cf. Fig. 2) are of the same order of magnitude as those determined experimentally (see, e.g., Ref. 27).

B. Work-Function Minimum

From each of the calculated curves of $\Phi(N)$ (two of which were shown in Fig. 2), we obtain a value of Φ_{min} . Since each curve corresponds to a particular choice of d , we obtain values for the function $\Phi_{\text{min}}(d)$ in this way. These are plotted in Fig. 3, with the points joined by a smooth curve. Recent experimental Φ_{min} values^{7, 27, 31, 32, 34-42} for each alkali A are put on the graph at $d=d_A$. The agreement between theory and experiment is good, both in the trend from alkali to alkali (i.e., in slope on the graph), and in absolute value. This suggests that our procedure for choosing d for each adsorbate is reasonable. Also, we see that the degree of dependence of our model calculations on d is just what might be expected on the basis of the experimental data. Note that we have only to shift the experi-

mental points horizontally on the graph to consider other choices for d .

C. Initial Slope of Work-Function-vs-Coverage Curve

An often-cited experimental quantity is the slope of the $\Phi(N)$ curve at zero coverage. The experimental determination of $\Phi'(0)$ requires, of course, measurements of N on an absolute scale, and as a result, there are fewer such determinations than there are of Φ_{min} . In the form $\Phi'(0)/4\pi$, this quantity is frequently called the zero-coverage (or initial) dipole moment⁴³ (see Sec. IV B). While it plays no basic theoretical role in the present treatment, the dipole moment is of central importance in discussions based on Langmuir's classical picture of alkali adsorption.⁴ We refer to the Appendix for a discussion of why our model, intended primarily for use at higher coverages, should still provide a reasonably satisfactory account of this quantity.

A curve of $-\Phi'(0)/4\pi$ vs d was derived from the calculated $\Phi(N)$ results in the same way that a plot of $\Phi_{\text{min}}(d)$ was obtained above. This curve (whose linearity is discussed in Sec. IV C), and the experi-

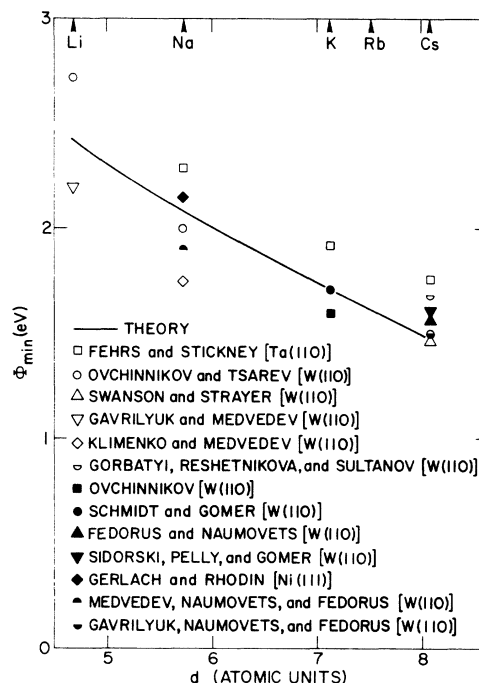


FIG. 3. Comparison between theoretical results and recent experimental data (Refs. 7, 27, 31, 32, 34-42) for Φ_{min} . The way in which the data were placed along the d axis is described in the text. The experimental substrates are specified in brackets; the text presents arguments for the relative unimportance of substrate choice to the value of Φ_{min} (considering, however, that the substrate is the most densely packed face of a high-work-function metal).

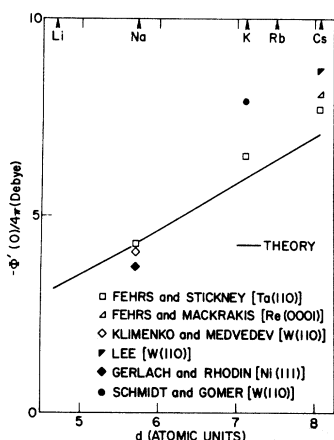


FIG. 4. Comparison between theoretical results and recent experimental data (Refs. 7, 27, 41, 44-47) for the zero-coverage dipole moment. Though the adsorption model is not designed for low coverages, it still yields reasonable values for this quantity (Appendix). See additional notes in caption of Fig. 3.

mental data^{7,27,41,44-47} on $\Phi'(0)$, are presented in Fig. 4 in just the same way that the results of theory and experiment were given in Fig. 3. Data for Cs adsorption on W(110) obtained using the field-emission method by Swanson and Strayer,³¹ Sidorski, Pelly, and Gomer,⁴⁰ and Gavrilyuk, Naumovets, and Fedorus,³² have been omitted from the figure because of problems related to determination of N (and of Φ_{sub}) which at present appear not fully to be resolved.⁴⁸ (These data have values considerably higher than the others shown for Cs in the figure.)

The degree of agreement between theory and experiment is difficult to assess, because of the lack of sufficient data, but it appears to be satisfactory. Note that the best agreement occurs for the case in which the experimental values agree most closely among themselves (Na adsorption).

D. Behavior of $\Phi(N)$ at Completion of a Full Layer of Adatoms

So far there is no imposed limit on the density of the adsorbate positive background in our model: \bar{n} in Eq. (2.4), and hence N , can take on any nonnegative value. Experimentally, as stated earlier, there is such a limit: When N reaches a certain value, a second layer of alkali atoms begins to form. We assume for the moment that second-layer formation does not commence until the first layer is full. Again as stated before, full first-layer coverage is found (for adsorption on the most densely packed substrate face) to be roughly equal to N_A , and it will be convenient, for purposes of discussion, to consider that it is exactly equal to N_A .

To study second-layer formulation theoretically, we replace the $n_s(x)$ of Eq. (2.4) by

$$n_s(x) = \begin{cases} \bar{n}_{\text{sub}}, & x \leq 0 \\ \bar{n}, & 0 < x \leq d \\ \bar{n}', & d < x \leq 2d \\ 0, & x > 2d \end{cases} \quad (3.1)$$

and impose a limit of \bar{n}_A on \bar{n} (which is reached when $N = N_A$). We compute $n(x)$, and hence Φ , just as before. Equation (2.5) for N remains unchanged in the range $0 \leq N \leq N_A$, but for $N_A < N \leq 2N_A$, we set $N = N_A + \bar{n}'d$ ($d = d_A$).

The derivative $\Phi'(N)$ now will be, in general, discontinuous at $N = N_A$. This behavior is shown by the $\Phi(N)$ curve computed for Na adsorption (i.e., for $d = d_{\text{Na}}$) in Fig. 5. A local maximum is seen to occur at $N = N_A$; we denote the maximum value by Φ_{max} . Experimentally, of course, this sharp structure may be expected to wash out if substantial second-layer formation⁴⁹ occurs while the first layer is being completed. This appears often to be the case, but there are a small number of reported Φ -vs-coverage curves that do show such a distinct maximum.^{34,38,42} An example of such a curve is shown in the inset in Fig. 5. In drawing a comparison between measured and calculated Φ_{max} values, we use measured values only from cases such as this. (Note that for the present purposes, an independent experimental determination of the coverage at which the first layer of adatoms is full is not required.)

To make a graphical comparison, similar to that

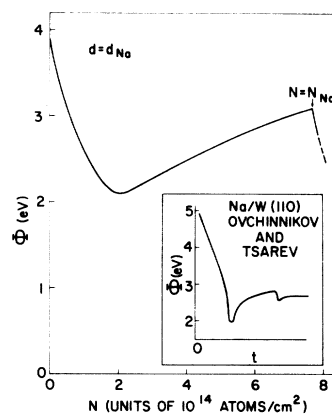


FIG. 5. Computed $\Phi(N)$ curve for Na adsorption, showing the maximum occurring at the commencement of second-layer formation. The inset shows an experimental curve (Ref. 34) exhibiting such a maximum. The abscissa of this curve is time of exposure t of the W(110) substrate to a flux of Na atoms: The coverage N is presumably a monotonically increasing though not linear function of t . [As explained in the text, no attempt was made to employ a model substrate whose work function would be as high as those of the substrates frequently used in the experiments (see caption of Fig. 2 for the effect of this on N_{min}).]

of Figs. 3 and 4, we note first that N_A is simply related to d_A [$N_A = 1/(\sqrt{2}d_A^2)$ if we take the alkalis to have a bcc structure]. Thus the calculated Φ_{\max} [i. e., $\Phi(N_A)$] is in fact a function only of d_A . We could, therefore, graph Φ_{\max} vs d just as we graphed Φ_{\min} vs d and $\Phi'(0)$ vs d earlier, placing experimental and theoretical points at $d = d_A$ and connecting the theoretical points with a smooth curve. It will, however, prove more convenient to use, instead of d_A , a quantity $r_s^{(A)}$, which is proportional to d_A and is defined by the relation $\frac{4}{3}\pi(r_s^{(A)})^3 = \bar{n}_A^{-1}$. Thus in Fig. 6 we label the abscissa r_s , place calculated and measured Φ_{\max} points at the appropriate $r_s = r_s^{(A)}$, and join the calculated points by a curve.

The experimental results fall close to this curve. No point is shown for Cs, because none of the measured curves for Cs adsorption exhibit a distinct maximum. (Neither is there a point for Rb, because as noted before, no recent measurements were found for this metal.) Experimental values for cases in which the maximum is largely washed out generally fall further below the curve.

It is often stated that the work function of a substrate with one full layer of an alkali A is equal to the work function of a bulk sample of A . This is very nearly true theoretically may be seen by comparing the solid and dashed curves in Fig. 6. The latter gives Φ vs r_s for the semiinfinite positive-background model discussed in Sec. II A (taking the reciprocal of the background density to be $\frac{4}{3}\pi r_s^3$). The two curves are seen to differ by no more than 0.05 eV.⁵⁰

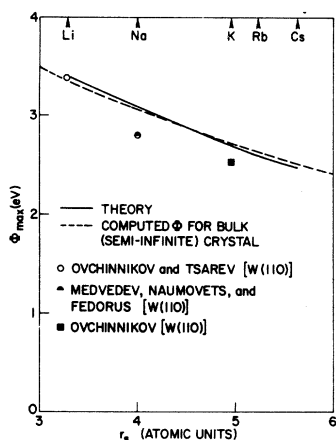


FIG. 6. Comparison between theoretical results (solid line) and recent experimental data (Refs. 34, 38, 42) for Φ_{\max} . The way in which the data were placed along the r_s axis is described in the text. Since Φ_{\max} in the model is equal to the full layer Φ , the assertion that the latter is approximately equal to the work function of a corresponding bulk sample may be verified theoretically by including the curve (dashed line) of Φ vs r_s for the semiinfinite-background model of a bulk metal.

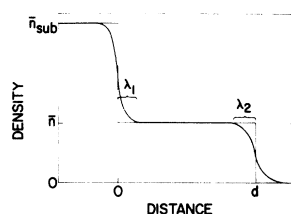


FIG. 7. Schematic representation of $n(x)$ when \bar{n} and d are sufficiently large for the substrate-adsorbate system to act like a bimetallic junction.

IV. GENERAL COMMENTS AND LIMITING CASES

In this section we examine several limiting cases of our model, with a view toward elucidating some of the major features of the results. It will be of particular interest to study, in this way, the question of why in fact there is a minimum in the work-function-vs-coverage curve. For these purposes, it is useful to again allow \bar{n} in the model to assume any nonnegative value, without formation of a second adsorbed layer. Also, in the first part of the discussion, it is convenient to think of Φ as a function of \bar{n} rather than of N as before.

We note immediately that for any value of d , Φ will equal Φ_{sub} when $\bar{n} = 0$ and again when $\bar{n} = \bar{n}_{\text{sub}}$. Thus we can demonstrate the presence of a minimum in the Φ -vs- \bar{n} curve either by showing that $d\Phi/d\bar{n} < 0$ at $\bar{n} = 0$ or that $d\Phi/d\bar{n} > 0$ at $\bar{n} = \bar{n}_{\text{sub}}$. It is quite another matter to show, in general, that the minimum occurs for $\bar{n} < \bar{n}_A$, when $d = d_A$ —we simply cite the fact that this occurrence was demonstrated above by actual computation.

In the following discussion, we consider the case in which d is very large (compared with substrate screening lengths), and examine how the behavior of Φ as a function of \bar{n} associated with this case persists down to smaller values of d ($\sim d_A$). For actual computations, we use the value of \bar{n}_{sub} employed earlier.

A. Substrate-Adsorbate System Viewed as Bimetallic Junction

We examine here the behavior of Φ as \bar{n} is lowered from \bar{n}_{sub} . For \bar{n} not too much smaller than \bar{n}_{sub} , our model is simply the model of a bimetallic junction, depicted schematically in Fig. 7, with a semiinfinite left-hand member and a finite- (though large-) thickness right-hand member.⁵¹ Φ is then the work function associated with a bulk sample (or, more precisely, with the semiinfinite-background model of such a sample) of mean electron density \bar{n} —the presence of the left-hand member has no effect on Φ . Since the work function of a bulk metal decreases as its mean electron density is lowered, we see immediately that $d\Phi/d\bar{n} > 0$ at $\bar{n} = \bar{n}_{\text{sub}}$, and hence that there must be a minimum in the Φ -vs- \bar{n} curve.

It is useful at this point to discuss briefly the way in which Eq. (2.2) applies to this bimetallic system. We may define $\bar{\mu}$ values separately for each

of the two members of the junction: $\bar{\mu}^{(\text{left})}$ and $\bar{\mu}^{(\text{right})}$. The mean $\bar{\mu}$ for the system as a whole is $\bar{\mu}^{(\text{left})}$, since the left member is semiinfinite; and so Eq. (2.2) may be written $\Phi = -\bar{\mu}^{(\text{left})} + \Delta\phi$. We can identify two distinct electrostatic double layers (cf. Fig. 7) that give rise to the potential difference $\Delta\phi$: one at the metal-metal interface, contributing $\Delta\phi_1$, and the other at the metal-vacuum interface, contributing $\Delta\phi_2$. The first layer simply makes the total chemical potentials in the two members equal, implying that $\Delta\phi_1 = \bar{\mu}_1^{(\text{left})} - \bar{\mu}^{(\text{right})}$. Hence,

$$\Phi = (-\bar{\mu}^{(\text{left})} + \Delta\phi_1) + \Delta\phi_2 = -\bar{\mu}^{(\text{right})} + \Delta\phi_2,$$

which exhibits Φ as the work function of a bulk sample having a mean electron density equal to that of the right-hand member.

We label by λ_1 the distance the first double layer extends into the right-hand positive background, and by λ_2 the distance the second layer extends into the background (see Fig. 7). Note that $\lambda_1 \sim \lambda_2 = O(\bar{n}^{-\gamma})$ (recall that atomic units are used), where roughly $\frac{1}{8} \lesssim \gamma \lesssim \frac{1}{3}$ (the Thomas-Fermi length is proportional to $\bar{n}^{-1/6}$; the Fermi wavelength is proportional to $\bar{n}^{-1/3}$). We assume \bar{n} to be small enough so that λ_1 is large relative to any lengths associated with the left-hand member.

It seems evident that as we decrease \bar{n} through the region defined by $d = O(\lambda_1 + \lambda_2)$, i. e., the region $\bar{n} = O(d^{-1/\gamma})$, that the right-hand member of the junction will cease, with regard to the work function, to behave like a bulk sample.⁵² Φ , then, need no longer decrease monotonically with \bar{n} : In particular, it becomes possible for the minimum to appear. Since d is large, Φ for the system will exhibit bulk work-function values associated with the density \bar{n} until \bar{n} is very small, implying that these Φ values, and hence, *a fortiori*, Φ_{min} , will themselves be quite small. For $\bar{n} \rightarrow 0$, Φ must, of course, return to Φ_{sub} .

We show schematically the expected behavior of the Φ -vs- \bar{n} curve for large d in Fig. 8. The ascending part of the curve (past the minimum region) is simply the bulk work function appropriate to a sample of mean electron density \bar{n} . The way in which this behavior persists for smaller values of d is illustrated by including the Na and Cs curves of Fig. 2, here with \bar{n} instead of N as the abscissa. Also included is the trivial curve for the opposite limiting case of $d=0$.

The above discussion provides a framework for understanding several important features of the experimental and theoretical $\Phi(N)$ curves for alkali adsorption. The first is the fact that there is indeed a minimum. The second is the decrease of Φ_{min} along the series Li, Na, K, Rb, Cs, i. e., with increasing d in our model (see Fig. 8). The third is that Φ_{min} is not strongly dependent on Φ_{sub} —this

is understandable if we consider the fact that the region of the minimum borders on the density range in which the adsorbate behaves, with regard to Φ , like a bulk sample.⁵³

B. Analogy with Langmuir Model

Let the symbol δ here indicate changes with respect to the bare-substrate case. Then we may write [using Eqs. (2.2) and (2.3)]

$$\delta\Phi = 4\pi aN, \quad (4.1)$$

with

$$a = N^{-1} \int_{-\infty}^{\infty} dx x [\delta n(x) - \delta n_+(x)]. \quad (4.2)$$

Clearly a is the separation of the centers of gravity of $\delta n(x)$ and $\delta n_+(x)$. [The function $\delta n_+(x)$ is, of course, simply the adsorbate background density, with center of gravity at $x = \frac{1}{2}d$ for coverages below a full layer (recall that the boundary of the substrate background is at $x=0$).] The quantity a functions very much in the present analysis as the dipole moment p did in the Langmuir picture. Note that the zero-coverage limit of a [$a(0)$] is just the expression $\Phi'(0)/4\pi$ which was discussed in Sec. III C.

Figure 9 shows $\delta n(x)$ for the case $d = d_{\text{Cs}}$ studied above, both for small \bar{n} and for $\bar{n} = \bar{n}_{\text{Cs}}$. Figure 10 shows the $a(N)$ associated with this case, over the range $0 \leq N \leq N_{\text{Cs}}$. Note that when $\bar{n} = \bar{n}_{\text{sub}}$, a must be zero (this occurs far off scale to the right in Fig. 10).

In terms of Eq. (4.1), the minimum in $\Phi(N)$ occurs when

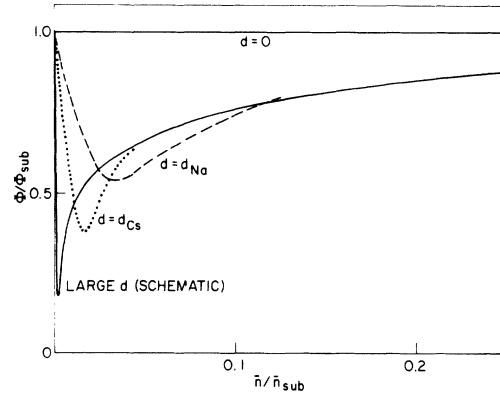


FIG. 8. This figure shows the way in which the model Φ -vs- \bar{n} curve depends upon d (second-layer formation excluded). Values of Φ for Na and Cs adsorption were computed only up to $\bar{n} = \bar{n}_A$. To the right of the general region of its minimum, the large- d curve is just a plot of work function vs background density for the semi-infinite-background model of a bulk sample (see text). All curves must meet at $\Phi = \Phi_{\text{sub}}$ when $\bar{n} = \bar{n}_{\text{sub}}$. Note the way in which the curves for alkali adsorption represent cases intermediate between those of large d and $d=0$; note in particular the decrease of Φ_{min} with an increase in d .

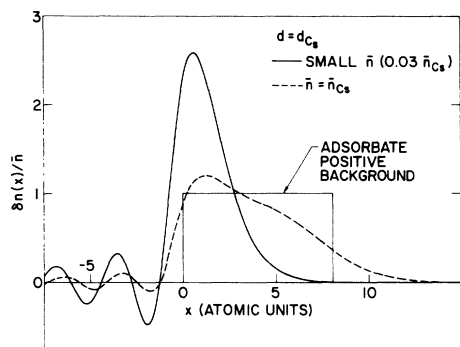


FIG. 9. Graphs of $\delta n(x)$ for small and full layer \bar{n} (Cs adsorption model). The small \bar{n} $\delta n(x)$ is nearly identical in shape to the change which would be induced in the bare-substrate electron density by a weak uniform electric field normal to the surface. As \bar{n} increases, the center of gravity of $\delta n(x)$ moves toward the right (and reaches the center of the adsorbate background when $\bar{n} = \bar{n}_{\text{sub}}$, excluding second-layer formation).

$$\frac{dN}{N} + \frac{da}{a} = 0,$$

that is, when the relative increase in the number of adsorbed atoms (dN/N) is offset by the decrease in the relative degree of electronic charge transfer away from the adsorbate positive charge (da/a).

C. Substrate-Adsorbate System Viewed as a Metal in Presence of Applied Electric Field

In this section we study the behavior of Φ as \bar{n} is raised from zero. We begin by imagining that the adsorbate positive background has been displaced a distance Δ to the right of the substrate background [i. e., we take $n_s(x)$ to have the form given in Eq. (2.6)]. We take Δ to be large compared with substrate screening lengths. For this case, with \bar{n} sufficiently small, it may easily be verified that it is energetically more favorable for the electrons to be in the vicinity of the substrate rather than the adsorbate background slab. This slab, then, acts simply as the source of a uniform electric field that perturbs the substrate. The field has a magnitude $\mathcal{E} = 4\pi\bar{n}d$, and is, of course, directed along the x axis. We will denote by x_0 the center of gravity of the charge distribution induced in the substrate by this field, in the $\mathcal{E} \rightarrow 0$ limit.

Graphs of such charge distributions are shown (for small \mathcal{E}) in Fig. 3 of Ref. 18. The distributions are localized within a few atomic units of the substrate background boundary. Relative to this boundary, $x_0 = +1.5$ atomic units for our choice of \bar{n}_{sub} (changing \bar{n}_{sub} within the metallic density range, however, does not change x_0 very much).

We now reduce Δ to zero. Because d has been taken to be large, most of the adsorbate background

still lies well away from the substrate. Thus we expect that this background will continue, to a good approximation, just to act as the source of a field, and that $\delta n(x)$ will resemble a field-induced charge distribution. Figure 9 (as noted before) shows $\delta n(x)$ at low \bar{n} for the case $d = d_{\text{Cs}}$. Even though this d value is not particularly large, a comparison of this distribution with that induced in the bare substrate by a weak field¹⁸ shows the two to be nearly identical.

We expect, therefore, for large d and for sufficiently small \bar{n} , that

$$N^{-1} \int_{-\infty}^{\infty} dx x \delta n(x) \approx x_0.$$

This implies that we can write the zero-coverage dipole moment, using Eq. (4.2), as

$$a(0) \approx x_0 - \frac{1}{2}d. \quad (4.3)$$

This equation has several implications of interest to us. First (since d is large) it is immediately clear that $a(0) < 0$, implying that $\Phi'(0)$ (and hence $d\Phi/d\bar{n}$ at $\bar{n} = 0$) is negative; this in turn means that there is necessarily a minimum in the Φ -vs- \bar{n} curve. Second, $\Phi'(0)$ varies linearly with d for large d ; Fig. 4 shows that this linear variation persists into the $d \sim d_A$ range.⁵⁴ Third, since it is found that x_0 is not strongly dependent on \bar{n}_{sub} ,¹⁸ $\Phi'(0)$ will not vary substantially with Φ_{sub} (for large d). A sample calculation (with $d = d_{\text{Na}}$) in which \bar{n}_{sub} was changed indicates that this behavior too persists for $d \sim d_A$. The degree to which the experimental data given in Fig. 4 shows an independence of $\Phi'(0)$ from Φ_{sub} is difficult to assess, since the number of measurements on different substrates is so small.

As \bar{n} increases past very small values, the electric field to which we have been comparing the effect of the adsorbate background grows so large that the response of the substrate to it becomes strongly nonlinear. This corresponds to a substantial shift in the induced-charge center of gravity (cf. Fig. 10), and to the onset of the region in which the work-function minimum occurs.

ACKNOWLEDGMENTS

It is a pleasure to thank M. C. Gutzwiller and

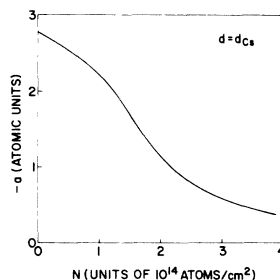


FIG. 10. Graph of a as a function of N for Cs adsorption model (values are shown only for $N \leq N_{\text{Cs}}$). Note that a must be exactly zero, excluding second-layer formation, when $N = \bar{n}_{\text{sub}}d$ (this occurs far off scale).

T. N. Rhodin for a number of helpful discussions.

APPENDIX: IMPORTANCE OF DISCRETE CHARACTER OF ADSORBATE IONIC CHARGE

In this Appendix, we consider briefly how severe an approximation it is to replace the array of adsorbate ions by a homogeneous positive background. Let $\delta n_1(\vec{r})$ be the difference between the self-consistent electron density in the presence of the adsorbed atoms and the self-consistent density in their absence. The distribution $\delta n_1(\vec{r})$ will, of course, be localized in regions of the surface near the ions. If we smear out the ionic charge parallel to the surface, then $\delta n_1(\vec{r})$ will be smeared out into a distribution $\delta n_2(x)$. We may think of adsorption, therefore, simply as the addition to the bare substrate of a charge configuration consisting, in one case, of an electron distribution of density $\delta n_1(\vec{r})$ plus the array of ions, and, in the other (model) case, of a distribution $\delta n_2(x)$ plus the smeared-out background. We refer to the first configuration as localized, and to the second as extended.

We note at this point that the only property of the added charge configurations that affects Φ is their dipole moment per unit area, or, for fixed coverage, the separation in centers of gravity of (added) negative and positive charge (cf. proof in Sec. II of Ref. 18). If these separations are the same for the two configurations, then the associated work-function changes will be the same. The localized and extended configurations will have very different energies (per adatom), however, particularly for low coverages, and as a result, our model does not account properly for low-coverage heats of adsorption.

Since we replace the ionic charge by a positive charge distribution that has its center of gravity at the ion position, it is clear that to see whether this

replacement affects Φ , all we need to consider is the question of whether the centers of gravity of $\delta n_1(\vec{r})$ and $\delta n_2(x)$ are the same. For purposes of further discussion, we examine the simplified case of point positive charges that are smeared out into a sheet (parallel to the surface), instead of the more complex case of ions, with their associated pseudopotentials, that are smeared into a slab.⁵⁵ For convenience, we also confine ourselves to speaking of the case of a single atom adsorbed on the surface (extreme low-coverage limit).

The point-charge density distribution may be Fourier-analyzed in directions parallel to the surface (we denote the associated transform variable by \vec{Q}), leading to the view of this distribution as a superposition of charge sheets whose densities vary in the plane of the sheet as $e^{i\vec{Q}\cdot\vec{R}}$ [$\vec{R}\equiv(y, z)$]. Similarly, the distribution $\delta n_1(\vec{r})$ may be Fourier-analyzed along \vec{R} . Note that it is only the $\vec{Q}=0$ component of δn_1 that affects its center of gravity.

If the point charge represents a small enough perturbation on the bare substrate (in particular if it is far enough away), then the various \vec{Q} components of the response will be decoupled from one another (linear response). The $\vec{Q}=0$ component of $\delta n_1(\vec{r})$ will represent the response only to the $\vec{Q}=0$ component of the point charge, but since the latter is just the uniformly smeared-out sheet we introduced above, it is clear that in this case the centers of gravity of $\delta n_1(\vec{r})$ and $\delta n_2(x)$ will be the same.

The question of the degree to which the substrate, in fact, responds linearly to a unit point charge at a given distance is very difficult to answer with any accuracy. No quantum-mechanical study of the nonlinear response properties of a metal surface is now available. We note only that the linear-response approximation in studying an ion near a surface is in common use,⁵⁶ and that the average d_A is larger than substrate screening lengths.⁵⁷

¹H. E. Ives, *Astrophys. J.* **60**, 209 (1924).

²I. Langmuir and K. H. Kingdon, *Proc. Roy. Soc. (London)* **A107**, 61 (1925).

³J. A. Becker, *Phys. Rev.* **28**, 341 (1926).

⁴I. Langmuir, *J. Am. Chem. Soc.* **54**, 2798 (1932).

⁵R. W. Gurney, *Phys. Rev.* **47**, 479 (1935).

⁶A. J. Bennett and L. M. Falicov, *Phys. Rev.* **151**, 512 (1966).

⁷L. D. Schmidt and R. Gomer, *J. Chem. Phys.* **45**, 1605 (1966).

⁸J. W. Gadzuk, in *Structure and Chemistry of Solid Surfaces*, edited by G. A. Somorjai (Wiley, New York, 1969). (See references in this paper to earlier work by the same author.)

⁹T. B. Grimley, *J. Vac. Sci. Technol.* **8**, 31 (1971).

¹⁰M. Remy, *J. Chem. Phys.* **53**, 2487 (1970).

¹¹J. W. Gadzuk, J. K. Hartman, and T. N. Rhodin, *Phys. Rev. B* **4**, 241 (1971).

¹²See also D. M. Newns, *Phys. Rev.* **178**, 1123 (1969);

Phys. Letters **33A**, 43 (1970); *Phys. Rev. Letters* **25**, 1575 (1970); G. Allan and P. Lenglar, *J. Phys. (Paris)*, Suppl. C, 1 (1970); K. F. Wojciechowski, *Acta Phys. Polon.* **29**, 119 (1966); **33**, 363 (1968).

¹³T. B. Grimley, *Proc. Phys. Soc.* **90**, 751 (1967); **92**, 776 (1967); *J. Phys. C* **3**, 1934 (1970); T. B. Grimley and S. M. Walker, *Surface Sci.* **14**, 395 (1969); A. J. Bennett, *J. Chem. Phys.* **49**, 1340 (1968).

¹⁴See, however, the phenomenological studies of E. P. Gyftopoulos and J. D. Levine, *J. Appl. Phys.* **33**, 67 (1962); and E. P. Gyftopoulos and D. Steiner, Report of the Twenty-Seventh Annual conference on Physical Electronics, Cambridge, Mass., 1967, p. 169 (unpublished). See also N. S. Razor and C. Warner, *J. Appl. Phys.* **35**, 2589 (1964).

¹⁵P. Hohenberg and W. Kohn, *Phys. Rev.* **136**, B864 (1964); W. Kohn and L. J. Sham, *ibid.* **140**, A1133 (1965).

¹⁶N. D. Lang, *Solid State Commun.* **7**, 1047 (1969).

¹⁷N. D. Lang and W. Kohn, Phys. Rev. B 1, 4555 (1970).

¹⁸N. D. Lang and W. Kohn, Phys. Rev. B 3, 1215 (1971).

¹⁹See also J. R. Smith, Phys. Rev. 181, 522 (1969); A. J. Bennett and C. B. Duke, in Ref. 8; J. Bardeen, Phys. Rev. 49, 653 (1936).

²⁰A preliminary account of this work was given in N. D. Lang, Solid State Commun. 9, 1015 (1971).

²¹Atomic units, with $|e| = m = \hbar = 1$, are used in this paper.

²²See in this connection R. Smoluchowski, Phys. Rev. 60, 661 (1941); J. R. Smith, Phys. Rev. Letters 25, 1023 (1970); and to be published.

²³For simplicity of discussion, we neglect possible changes in d_{sub} near the surface; calculation suggests that these changes are small in any case (see Appendix E of Ref. 17).

²⁴Compare with J. W. Gadzuk, Phys. Rev. B 1, 1267 (1970). Note also here the finding of A. G. Fedorus and A. G. Naumovets [Surface Sci. 21, 426 (1970)] that the long-range order of the ions in an adsorbed alkali film has a negligible effect on the work function.

²⁵As in the case of the bare-surface model, the difference between the potential due to the adsorbate ions and that due to the corresponding background slab may be viewed as a small perturbation δv . This is only possible if the sheet of ions is at the slab center, since otherwise δv will not vanish at $\pm \infty$.

²⁶The only rigorous way to choose a correct d for each N (or \bar{n}) is to use substrate-adsorbate distances determined either by actual measurement (such data are not now available) or by minimizing the adsorption energy theoretically. It is pointed out in the Appendix why the present model is unsuited to a calculation of energies of adsorption. No such minimization has been carried out using the Gurney model either—see the discussion of this point in Ref. 11. The present picture, with a fixed d , will be seen, however, to provide a quite satisfactory elucidation of the observed work-function behavior. (The variation of Φ as both \bar{n} and d are changed can be studied, if this is of interest, simply by interpolating in a graph such as that of Fig. 8, which presents Φ -vs- \bar{n} curves for several d values.)

²⁷D. L. Fehrs and R. E. Stickney, Surface Sci. 24, 309 (1971).

²⁸R. L. Gerlach and T. N. Rhodin, Surface Sci. 17, 32 (1969).

²⁹Note particularly in this connection the discussion of Sec. III D.

³⁰In atomic units, $d_{\text{Li}} = 4.68$, $d_{\text{Na}} = 5.73$, $d_{\text{K}} = 7.13$, $d_{\text{Rb}} = 7.51$, $d_{\text{Cs}} = 8.08$ (assuming a bcc structure for the alkalis). (Were we to take the alkalis to be fcc, these distances would change by less than 3%.)

³¹L. W. Swanson and R. W. Strayer, J. Chem. Phys. 48, 2421 (1968).

³²V. M. Gavrilyuk, A. G. Naumovets, and A. G. Fedorus, Zh. Eksperim. i Teor. Fiz. 51, 1332 (1966) [Sov. Phys. JETP 24, 899 (1967)].

³³Sample calculation for Na adsorption with $r_{\text{a}}^{(\text{sub})} = 3$ instead of 2 a.u.

³⁴A. P. Ovchinnikov and B. M. Tsarev, Fiz. Tverd. Tela 9, 3512 (1967) (Li adsorption); 9, 1927 (1967) (Na adsorption); 8, 1493 (1966) (Cs adsorption) [Sov. Phys. Solid State 9, 2766 (1968); 9, 1519 (1968); 8, 1187 (1966)].

³⁵V. M. Gavrilyuk and V. K. Medvedev, Fiz. Tverd.

Tela 8, 1811 (1966) [Sov. Phys. Solid State 8, 1439 (1966)].

³⁶E. V. Klimenko and V. K. Medvedev, Fiz. Tverd. Tela 10, 1986 (1968) [Sov. Phys. Solid State 10, 1562 (1969)].

³⁷N. A. Gorbatyi, L. V. Reshetnikova, and V. M. Sultanov, Fiz. Tverd. Tela 10, 1185 (1968) [Sov. Phys. Solid State 10, 940 (1968)].

³⁸A. P. Ovchinnikov, Fiz. Tverd. Tela 9, 628 (1967) [Sov. Phys. Solid State 9, 483 (1967)].

³⁹A. G. Fedorus and A. G. Naumovets, Surface Sci. 21, 426 (1970).

⁴⁰Z. Sidorowski, I. Pelly, and R. Gomer, J. Chem. Phys. 50, 2382 (1969).

⁴¹R. L. Gerlach and T. N. Rhodin, Surface Sci. 19, 403 (1970); measured work function for bare Ni (111) face was 5.20 eV (private communication).

⁴²V. K. Medvedev, A. G. Naumovets, and A. G. Fedorus, Fiz. Tverd. Tela 12, 375 (1970) [Sov. Phys. Solid State 12, 301 (1970)].

⁴³Some writers apply this term to the quantity $\Phi'(0)/2\pi$; this will not be done here.

⁴⁴D. L. Fehrs and M. S. Mackrakis, Bull. Am. Phys. Soc. 15, 391 (1970); and private communication. I would like to thank Dr. Fehrs for making these data available to me.

⁴⁵Reference 36, as analyzed by E. V. Klimenko and A. G. Naumovets [Surface Sci. 14, 141 (1969)].

⁴⁶T. J. Lee, Ph.D. thesis (University of Southampton, England, 1967) (unpublished), as quoted in Ref. 8.

⁴⁷No attempt was made to extract values for $\Phi'(0)$ from measured $\Phi(N)$ curves; only values that were computed by the experimentalists themselves were used.

⁴⁸I would like to thank L. W. Swanson for discussing this matter with me.

⁴⁹R. D. Young and D. C. Schubert, J. Chem. Phys. 42, 3943 (1965).

⁵⁰We note at this point that observed Φ anisotropies for full-layer (and multilayer) alkali adsorption [see, e.g., T. J. Lee, B. H. Blott, and B. J. Hopkins, Appl. Phys. Letters 11, 361 (1967)] can be understood theoretically in terms of the analysis of Ref. 18.

⁵¹For a discussion of the electronic structure of bimetallic junctions (with both members semi-infinite) see A. J. Bennett and C. B. Duke, Phys. Rev. 160, 541 (1967); 162, 578 (1967).

⁵²See, in connection with this discussion, L. N. Dobretsov and T. L. Matskevich, Zh. Tekhn. Fiz. 36, 1449 (1966) [Sov. Phys. Tech. Phys. 11, 1081 (1967)].

⁵³The computation of Ref. 33 led to a change of Φ_{min} which was less than 15% as great as the change in Φ_{sub} .

⁵⁴Equation (4.3) yields a value for $\Phi'(0)$ whose error for $d \sim d_A$ (relative to the computed value) ranges from less than 10% for Cs adsorption to 30% for Li adsorption.

⁵⁵The pseudopotential core of an alkali ion located at $x = \frac{1}{2}d_A$ turns out to be outside of much of the bare-substrate electron distribution, and so our replacement of the ion by a point charge in this discussion is a reasonable approximation. Also, the analysis of Sec. IV C suggests that the responses of the substrate to a charge slab in the region $0 \leq x \leq d_A$ and to a charge sheet at $x = \frac{1}{2}d_A$ should be very similar.

⁵⁶See discussion in D. M. Newns, Phys. Rev. B 1, 3304 (1970).

⁵⁷We add to this Appendix the note that a sample calculation for Na adsorption, in which the effect of the adsor-